FcεRI-mediated Association of 6-μm Beads with RBL-2H3 Mast Cells Results in Exclusion of Signaling Proteins from the Forming Phagosome and Abrogation of Normal Downstream Signaling

Lynda Pierini, David Holowka, and Barbara Baird

Department of Chemistry, Cornell University, Ithaca, New York 14853-1301

Abstract. Cells of the mucosal mast cell line, RBL-2H3, are normally stimulated to degranulate after aggregation of high affinity receptors for IgE (FcεRI) by soluble cross-linking ligands. This cellular degranulation process requires sustained elevation of cytoplasmic Ca^{2+}. In this study, we investigated the response of RBL-2H3 cells to 6-μm beads coated with IgE-specific ligands. These ligand-coated beads cause only small, transient Ca^{2+} responses, even though the same ligands added in soluble form cause larger, more sustained Ca^{2+} responses. The ligand-coated 6-μm beads also fail to stimulate significant degranulation of RBL-2H3 cells, whereas much larger ligand-coated Sepharose beads stimulate ample degranulation. Confocal fluorescence microscopy shows that the 6-μm beads (but not the Sepharose beads) are phagocytosed by RBL-2H3 cells and that, beginning with the initial stages of bead engulfment, there is exclusion of many plasma membrane components from the 6-μm bead/cell interface, including $p53/56^{lyn}$ and several other markers for detergent-resistant membrane domains, as well as an integrin and unliganded IgE-FcεRI. The fluorescent lipid probe $DiIC_{16}$ is a marker for the membrane domains that is excluded from the cell/bead interface, whereas a structural analogue, fast DiI, which differs from $DiIC_{16}$ by the presence of unsaturated acyl chains, is not substantially excluded from the interface. None of these components are excluded from the interface of RBL-2H3 cells and the large Sepharose beads. Additional confocal microscopy analysis indicates that microfilaments are involved in the exclusion of plasma membrane components from the cell/bead interface. These results suggest that initiation of phagocytosis diverts normal signaling pathways in a cytoskeleton-driven membrane clearance process that alters the physiological response of the cells.

AGGREGATION of FcεRI, the high affinity receptor for IgE found predominantly on mast cells and basophils, stimulates a signaling cascade that leads to exocytosis of inflammatory mediators of the allergic response (5, 33). The signaling pathways initiated by FcεRI aggregation are similar to those initiated by aggregation of the T and B cell multichain immune recognition receptors (9, 23, 52). Some of the steps in these signaling pathways are phosphorylation of tyrosine residues in the immunoreceptor tyrosine activation motif (ITAM)[1] sequences of receptor cytoplasmic segments by src-family protein tyrosine kinases (PTKs), binding and activation of ZAP70/syk-family PTKs, phosphatidyl inositol hydrolysis, protein kinase C activation, and mobilization of intracellular Ca^{2+} (5, 43).

FcεRI is a multisubunit receptor comprising α, β, and a disulfide-linked pair of γ subunits (7). Whereas the α subunit contains the IgE binding site, the β and γ subunits contain the ITAMs and are involved in signal transduction. As the result of FcεRI aggregation, the src-family PTK $p53/56^{lyn}$ phosphorylates the tyrosines within the ITAMs, leading to recruitment of $p72^{syk}$ to the γ subunit (6, 26, 39, 44). The mechanism by which FcεRI aggregation leads to the earliest phosphorylation events, i.e., phosphorylation of β and γ by $p53/56^{lyn}$, is not completely understood (41). Likewise, coupling of tyrosine kinase activation and substrate phosphorylation to more downstream signaling events, including Ca^{2+} mobilization and stimulated exocytosis, is only partially understood (24).

We recently showed that a large fraction of the total cellular $p53/56^{lyn}$ associates with low-density Triton X-100

Address all correspondence to David Holowka and Barbara Baird, Department of Chemistry, Cornell University, Ithaca, NY 14853-1301. Tel.: (607) 255-4095. Fax: (607) 255-4137. E-mail: BAB13@cornell.edu

1. *Abbreviations used in this paper*: $DiIC_{16}$, 3, 3′-dihexadecylindocarbocyanine; DNP-BGG, bovine gamma globulin multiply conjugated to DNP; fast DiI, 3, 3′-dilinoleylindocarbocyanine; GPI, glycosylphosphatidylinositol; IgE_{biotin}, biotinylated IgE; ITAM, immunoreceptor tyrosine activation motif; PTK, protein tyrosine kinase; sAv, streptavidin; TNP, 2, 4, 6-trinitrophenyl; TX-100, Triton X-100.

(TX-100)–insoluble membrane domains isolated from the mucosal mast cell line RBL-2H3 and that the extent of this association increases after FcεRI-aggregation (17). We also observed that the fluorescent lipid probe 3,3′-dihexadecylindocarbocyanine ($DiIC_{16}$) labels membrane domains on the surface of RBL cells that coredistribute with aggregated FcεRI (49). In the same study, we found that these membrane domains can be similarly redistributed by aggregating α-galactocyl derivatives of a GD_{1b} ganglioside via a specific mAb, AA4 (4, 20). Importantly, these gangliosides, as well as the glycosyl phosphatidylinositol (GPI)-linked protein Thy-1, was found to coisolate with $p53/56^{lyn}$ in immunoprecipitates from TX-100–lysed cells (14, 34) and with the detergent-resistant membrane domains containing $p53/56^{lyn}$ (17), suggesting that the cell surface membrane domains observed with fluorescence microscopy are related to those structures isolated from TX-100–lysed cells. These studies led to our hypothesis that coalescence of membrane domains with aggregated FcεRI is functionally important because it allows communication of domain-associated signaling molecules with these aggregated receptors (17, 24).

In this study, we used fluorescence flow cytometry and confocal microscopy to investigate the capacity of ligand-coated, 6-μm-diam beads to bind IgE–FcεRI and stimulate RBL cells. We find that the beads elicit neither degranulation nor sustained Ca^{2+} responses from RBL cells. Instead, RBL cells phagocytose these beads, and this process causes physical segregation of membrane domain components from FcεRI at the cell/bead interface. The implications of these results for FcεRI-mediated signaling, as well as for plasma membrane structure, and phagocytosis, are discussed.

Materials and Methods

Purified Antibodies and Other Reagents

Mouse anti-rat Thy-1.1 mAb was obtained from PharMingen (San Diego, CA). Leu4, a mouse IgG mAb that recognizes the ε subunit of the CD3 complex of the TCR, was obtained from Becton-Dickinson Immunocytometry Sys. (San Jose, CA). The mouse mAb, AA4, which recognizes α-galactosyl derivatives of the ganglioside GD_{1b} (20) was from Dr. R. Siraganian (National Institutes of Health, Bethesda, MD). The mouse mAb TA2, which recognizes the α subunit of rat VLA4 integrin (27), was from Dr. T. Issekutz (Toronto Hospital, Toronto, Ontario). Anti–2,4-dinitrophenyl mouse IgE mAb (30) was purified as described previously (25). Fluorescein 5′-isothiocyanate-labeled biotinylated IgE ($FITC\text{-}IgE_{biotin}$) was prepared by first conjugating biotin to IgE as previously described (17) and then, after extensive dialysis against PBS, labeling with FITC as previously described (16). The resulting $FITC\text{-}IgE_{biotin}$ contained approximately nine fluoresceins per IgE as determined by UV-vis absorption spectroscopy. Biotinylated Leu4 was prepared similarly to biotinylated IgE (17). The multivalent antigens, 2,4-dinitrophenylated bovine serum albumin (DNP-BSA) and 2,4-dinitrophenylated bovine gamma globulin (DNP-BGG), contained 16–18 DNP groups per BSA and 24–27 DNP groups per BGG, respectively, as determined by UV-vis spectroscopy, and were prepared as described previously (51). The amino reactive carbocyanine dye, Cy3, was conjugated to antibodies or BGG following the procedure provided by the manufacturer (Biological Detection Systems, Pittsburgh, PA).

The streptavidin (sAv; Sigma Chemical Co., St. Louis, MO)-coated beads were prepared by covalently conjugating 20 μg streptavidin to 0.5 mL of 2.5% (wt/vol) carboxylated microspheres (6-μm diam, carboxylated, latex-coated polystyrene; Polysciences, Inc., Warrington, PA) with a carbodiimide reaction, as previously described (22). Streptavidin-coated fluorescent beads, used for flow cytometry experiments, were prepared as above except with 6-μm carboxylated beads that had red fluorescent dye incorporated (Polysciences Inc.).

Fluorescent DNP-BGG–coated 6-μm beads were prepared by conjugating 160 μg of DNP-BGG premixed with 240 μg Cy3-conjugated BGG to 0.5 ml of 2.5% (wt/vol) carboxylated beads with the same procedure described above. Anti-rat IgE (IgE_{rat})–coated 6-μm beads were prepared by first conjugating 30 μg of goat anti-mouse kappa IgG (Fisher Scientific, Pittsburgh, PA) to fluorescent carboxylated beads and then successively incubating these beads (8×10^7/ml) with 10 μg/ml anti-rat ε IgE mAb (A2; reference 11) and then 33 μg/ml nonspecific mouse IgG (Cappel/Organon Teknika, Durham, NC) for 45 min at room temperature, followed by a wash with buffered saline solution (BSS: 135 mM NaCl, 5.0 mM KCl, 1.8 mM $CaCl_2$, 1.0 mM $MgCl_2$, 5.6 mm glucose, 1 mg/mL BSA, and 20 mM Hepes, pH 7.4).

2,4,6-trinitrophenyl (TNP)–derivatized beads were prepared by reacting cyanogen bromide-activated 100 μm Sepharose 4B beads (Sigma Chemical Co.) with ε-TNP-L-lysine hydrochloride (Research Organics Inc., Cleveland, OH). 15 g of cyanogen bromide–activated Sepharose 4B beads were swelled in 1 mM HCl for 15 min and then washed with several volumes of 1 mM HCl, followed by a wash with 0.1 M $NaHCO_3$, pH 8.3. 50 mg ε-TNP-L-lysine hydrochloride in 75 ml of 0.1 M $NaHCO_3$ was added to the swollen beads. After a 2 h incubation at room temperature, the beads were further incubated at 4°C overnight. The beads were then washed once with 0.2 M glycine, followed by incubation for 2 h at room temperature in 0.2 M glycine to block any remaining active sites. They were stored in 0.2 M H_3BO_3, 0.16 M NaCl, pH 8.5.

Cells

RBL-2H3 cells (3) were maintained in monolayer culture in Minimum Essential Medium supplemented with 10% fetal bovine serum (Atlanta Biologicals, Norcross, GA), 1 ml/liter mito+ serum extender (Collaborative Biomedical Products, Bedford, MA), and 10 μg/ml gentamicin. Typically, cells were used 3–5 d after passage.

HPB-ALL cells, a human leukemia T cell line, were maintained in RPMI 1640 supplemented with 10% fetal bovine serum, 1 ml/liter mito+ serum extender, 50 μg/ml streptomycin sulfate, 50 U/ml penicillin, and 1 mM sodium pyruvate. T cells were grown at 37°C in a 5% CO_2 incubator to a concentration of $1–3 \times 10^5$ cells/ml. All tissue culture reagents were obtained from GIBCO BRL (Gaithersburg, MD) unless otherwise noted.

β-Hexosaminidase Release Assay

After overnight incubation with 1 μg/ml IgE, adherent RBL cells were harvested by treatment with 1.5 mM EDTA, 135 mM NaCl, 5 mM KCl, and 20 mM Hepes, pH 7.4, for 10 min and then diluted with BSS. Harvested cells were sedimented at 200 *g* for 8–10 min, washed once in BSS and then resuspended at 4×10^6 cells/ml in BSS with 1 mg/ml BSA. Aliquots of cells were diluted fourfold with prewarmed solutions of stimulating ligands, including freshly washed sAv-coated beads and TNP-derivatized beads and then incubated for 60 min at 37°C on a rotator. The samples were centrifuged at 9,000 *g* for 2 min to sediment the cells before an aliquot of supernatant was assayed for β-hexosaminidase content by a colorimetric enzyme assay (46). Briefly, 50 μl of sample supernatant was incubated with 200 μl of 1 mM enzyme substrate (p-nitrophenyl-*N*-acetyl-β-D-glucosaminide) in 0.05 M citrate buffer (pH 4.5) for 1 h at 37°C in a 5% CO_2 incubator. The reaction was quenched by addition of 500 μl of 0.1 M sodium carbonate buffer. β-Hexosaminidase concentration was determined by measuring OD at 400 nm and comparing to total β-hexosaminidase released by cells lysed in 0.5% TX-100. The number of 6-μm beads conjugated per cell, as well as the number of cells conjugated per TNP bead (100-μm diam), was determined by microscopy. Samples designated 1:1 cell/6-μm bead contained ~40% of the cells as conjugates with ~25% of these conjugates having >1 bead per cell (typically 2 beads/cell). Samples designated 3:1 cell/6-μm bead contained ~90% of the cells as conjugates with 54% of these conjugates having >1 bead per cell (typically >2 beads/cell but <5 beads/cell).

Flow Cytometry

Adherent RBL cells were incubated overnight with 1 μg/ml IgE_{biotin}. Cells were harvested as above and resuspended at 1×10^7 cells/ml in BSS with 0.25 mM sulfinpyrazone (Sigma Chemical Co.) and then loaded with indo-1/AM (Calbiochem-Novabiochem, San Diego, CA), a fluorescent Ca^{2+} indicator, as previously described (51). Briefly, 1 mg/ml indo-1 in DMSO was diluted 11-fold in newborn calf serum. 250 μl of this indo-1/AM solu-

tion was added to 3×10^7 cells. The cells were incubated for 1 min at 37°C and then diluted 7.5-fold in BSS with 0.25 mM sulfinpyrazone. After the cells were incubated for an additional 30 min at 37°C, they were washed two times, resuspended at 4×10^6 cells/ml in BSS with sulfinpyrazone, and placed on ice until use. HPB-ALL cells were washed once with BSS, resuspended at 1×10^7 cells/ml, and then loaded with indo-1 as above. Typically, for both RBL and HPB-ALL cells, 500 μl of 4×10^6 cells/ml in BSS were maintained with stirring at 37°C throughout an experiment. Additions of 10 μl of beads (~7×10^7 beads/ml) or soluble ligand were made at various times as indicated.

The cytoplasmic free Ca^{2+} levels of cell/bead conjugates and free cells were monitored simultaneously with a method previously described (22). In short, excitation of indo-1 (351.1–361.1-nm UV multiline) and of red fluorescent beads (514 nm) was achieved with the two Argon ion lasers (model Innova 90-4 and 90-5; Coherent, Inc., Palo Alto, CA) on a flow cytometer (model Epic 753; Coulter Corp., Hialeah, FL). The cell/bead population was gated separately from the free cell population based on size, with a solid state photodetector to measure forward angle light scatter, and on red fluorescence, with a PMT to measure emissions of >590 nm. The relative intracellular Ca^{2+} concentration ($[Ca^{2+}]_i$) was determined from the ratio of the fluorescence of Ca^{2+}-bound indo-1 (395 nm) to the fluorescence of free indo-1 (525 nm). Monitoring the fluorescence ratio corrects for differences in cell size and indo-1 loading. In these experiments, transit time of the cells and conjugates from the sample chamber to the detection point is 30–90 s.

Microscopy

Coverslips (22 × 22 mm, No. 1. Corning Glass Works, Corning, NY) were incubated with 20 mg/ml BSA in BSS for 30 min at 37°C. Suspended RBL cells were incubated with either excess FITC-IgE_{biotin} premixed with Cy3-IgE or excess FITC-IgE_{biotin} alone for at least 1 h at 37°C. Cells sensitized with FITC-IgE_{biotin} alone were further labeled by incubation for 30 min at 4°C with Cy3-conjugated mAbs specific for Thy-1 or the ganglioside GD_{1b} and then washed. BSA solution was removed from the coverslips before the addition of 200 μl of labeled RBL cells in suspension (2×10^6 cells/ml in BSS). Cells were allowed to settle and adhere for 10 min at room temperature. Cell supernatants were removed and replaced with a suspension of nonfluorescent sAv beads. After a 30-min incubation at room temperature, the coverslips were washed gently three times with PBS. Cells were fixed by addition of 3.7% formaldehyde in PBS and incubation for 20 min at room temperature, washed thoroughly with PBS containing 5% newborn calf serum (GIBCO BRL), and then permeabilized by addition of 0.1% TX-100 for 5 min at room temperature. Alternatively, to obtain maximal phagocytosis, suspended FITC-IgE_{biotin}–sensitized cells (4×10^6 cells/ml) were rotated with sAv beads (4×10^6 beads/ml) for 20 min at 37°C and then kept on ice until examined by confocal microscopy.

For some samples, polymerized actin or VLA4 integrin were labeled after permeabilization of the fixed, FITC-IgE_{biotin}–sensitized cells by addition of 0.1% TX-100. Permeabilized cell/bead conjugates were incubated with either 1 U/200 μl of rhodamine-phalloidin (Molecular Probes, Eugene, OR) or 4 μg/ml of anti–rat mAb VLA4 (TA2; reference 27), respectively, for 20 min at room temperature. After washing, anti-VLA4–labeled cells were incubated for 20 min at room temperature with 5 μg/ml Cy3-conjugated rabbit anti–mouse IgG (Fc specific; Jackson Immunochemicals, West Grove, PA) and then washed in PBS containing 1 mM EDTA and 10 mg/ml BSA.

For labeling $p53/56^{lyn}$, cells on coverslips were immersed in MeOH precooled to −20°C and then incubated at 4°C for 10 min followed by MeOH removal and drying with a stream of N_2. Cells were immediately rehydrated with PBS containing 1 mM EDTA and 10 mg/ml BSA and labeled by incubation with a 1:5,000 dilution of rabbit anti-lyn (Upstate Biotechnology Inc., Lake Placid, NY) or control antiserum in the same buffer, followed by washing and incubation with 5 μg/ml Cy3-conjugated goat anti–rabbit IgG (Fc specific; Jackson Immunochemical). Attempts to label $p53/56^{lyn}$ with the more standard fixation and permeabilization procedures described above resulted in much weaker specific staining with the anti-lyn antibody we used.

For labeling with 3,3′-dihexadecylindocarbocyanine ($DiIC_{16}$; Molecular Probes) or 3,3′-dilinoleylindocarbocyanine (fast DiI; Molecular Probes), 3 μl of 0.2 mg/ml $DiIC_{16}$ or 1 μl of 0.2 mg/ml fast DiI in MeOH was added to 125 μl of RBL cells (4×10^6 cells/ml in BSS). After a 1-min incubation at room temperature, the cells were incubated 10 min on ice, washed twice with cold BSS, and then plated onto coverslips as described above. Some images of cells labeled with either of the carbocyanine dyes were thresholded such that all of the lower 25% of the fluorescence intensity was set to the lowest allowable value (channel 0) and all of the upper 75% was set to the maximum allowable value (channel 255).

To study the coredistribution of AA4 with aggregated IgE–FcεRI complexes, suspended FITC-IgE–sensitized cells were incubated with Cy3-AA4 for 30 min at 37°C, and then washed twice with BSS. To cross-link IgE–FcεRI, cells (1.5×10^6 cells/ml) were incubated with 5 μg/ml biotinylated sheep anti-IgE(ε) (The Binding Site, San Diego, CA) for 1 h at 4°C. For further aggregation, the cells were washed twice with BSS, incubated with 50 μg/ml sAv for 30 min at 4°C, and then warmed at 37°C for 10 min. The cells were washed twice with PBS at room temperature and then formaldehyde fixed as described above.

All fixed microscopy samples were washed thoroughly before being mounted onto glass slides with 9 μl of 0.13 g/ml Airvol 205 (Air Products and Chemicals, Inc., Allentown, PA), 0.3 g/ml glycerol, 70 mM Tris, pH 8.5, and 15 mg/ml 1,4-diazabicyclo-[2.2.2] octane to reduce photobleaching.

Samples were imaged with an MRC 600 confocal system (BioRad, Cambridge, MA) in conjunction with a Zeiss Axiovert 10 microscope (Thornwood, NY). The 488- and 568-nm lines of a krypton-argon ion laser (Ion Laser Technology, Salt Lake City, UT), selected by a laser bandpass filter, were used for fluorescein and Cy3/DiI/rhodamine excitation, respectively. Fluorescein fluorescence was measured through a 522-nm dichroic filter, while Cy3/DiI/rhodamine fluorescence was measured through a 585-nm-long pass filter. A 63× achromatically corrected oil objective (NA 1.4) was used to acquire images. Fluorescein and Cy3/DiI/rhodamine images were collected sequentially with BioRad COMOS software.

Results

Ligands That Cross-link IgE–FcεRI Are Poor Activators of Ca^{2+} Responses and Cellular Degranulation When Attached to Cell-sized Beads

We previously showed that HPB-ALL human leukemia T cells exhibit strong, sustained Ca^{2+} responses when these cells form conjugates with 6-μm-diam beads coated with anti–T cell receptor (TCR) mAb (22). Fig. 1 *A* shows an example of this response as monitored by flow cytometry with cytoplasmic Ca^{2+} detected as the fluorescence ratio of indo-1 (395 nm/525 nm) and simultaneously measured for free cells and cell/bead conjugates. As conjugates begin to form at 37°C, the cytoplasmic Ca^{2+} of the bead-coupled cells increases to concentrations that are similar to the maximal response elicited by the same anti-TCR mAb when added in soluble form (data not shown). The response to the beads, which gradually decreases over the time period of 20 min, is generally more sustained than that observed with soluble anti-TCR mAb (22). For the experiment shown in Fig. 1 *A*, beads were coated with biotinylated anti-TCR via sAv that is covalently conjugated to the beads; the lack of any response in the free cells shows that there is no leakage of this ligand from the beads during the course of the experiment.

Fig. 1 *B* shows a comparable experiment with RBL cells in which biotinylated IgE is prebound to FcεRI on the cells, and conjugates are formed between these indo-1–loaded cells and the same sAv-coated 6-μm beads used for Fig. 1 *A*. Conjugate formation occurs with similar kinetics for both cell types, as shown by the lower curves (Δ) in Fig. 1, *A–D*. Under these conditions, virtually all of the conjugates are in a 1:1 ratio to minimize complex responses and clogging of the flow cytometer intake by large clusters of beads and cells. In control experiments, cells mixed with 6-μm beads that have been coated with an irrelevant Ab form <0.2% conjugates under the same conditions, indicating the specificity of the interactions represented in Fig. 1,

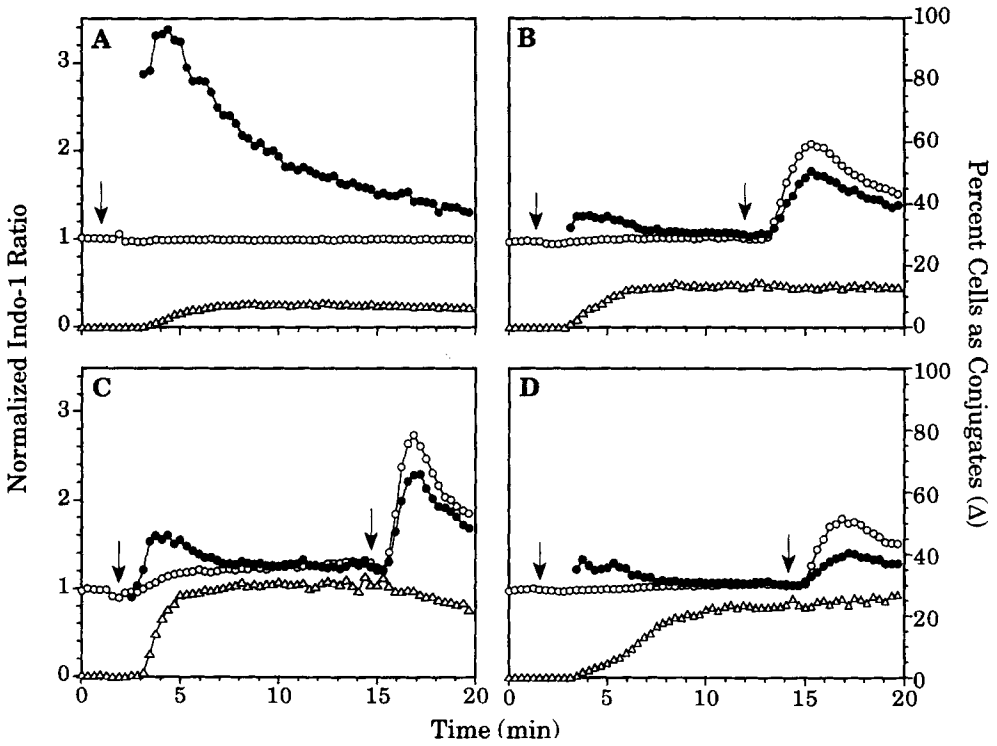

Figure 1. The Ca^{2+} response of HPB-ALL cells (*A*) and RBL cells (*B–D*) to ligand-coated 6-μm beads. The time course of conjugate formation is shown for each experiment as percent of cells in conjugates (Δ) at the bottom of each panel. The indo-1 ratio for free cells (○) and cell/bead conjugates (●) was monitored as a function of time. (*A*) Biotinylated anti-TCR bound to sAv beads was added to HPB-ALL cells at the arrow. (*B*) sAv beads were added to IgE_{biotin}-sensitized RBL cells at the first arrow, followed by the addition of 2 pM sAv at the second arrow. (*C*) DNP-BGG–coated beads were added to anti-DNP IgE-sensitized RBL cells at the first arrow, followed by the addition of 100 ng/ml DNP-BGG at the second arrow. (*D*) mAb A2-coated beads were added to IgE_{rat}-sensitized RBL cells at the first arrow, followed by the addition of 100 ng/ml A2 at the second arrow. For these experiments, the final concentrations of cells and beads were ~4 × 10^6/ml and ~1.4 × 10^6/ml, respectively.

B–D. The striking result illustrated in Fig. 1 *B* is that the Ca^{2+} response elicited by conjugate formation via FcεRI on RBL cells is usually small and always transient. The elevated Ca^{2+} levels in these cells return to the unstimulated cytosolic concentration in <10 min after initiation of conjugate formation. This contrasts with the stronger and more sustained Ca^{2+} response that is usually elicited from these cells by soluble FcεRI ligands, even when relatively low concentrations are used (29). This is illustrated in Fig. 1 *B*, in which the secondary addition of an extremely low dose of soluble sAv (2 pM) causes a moderately strong Ca^{2+} response in the free cells that is sustained for many tens of min (data not shown). This dose of soluble sAv causes a sustained response in the cell/bead conjugates that is larger than that initially elicited by the beads but is consistently smaller than that observed for the free cells. Under these conditions, a large fraction of the IgE_{biotin}–FcεRI is outside the cell/bead contact region (see below), so it appears that the aggregation of FcεRI at the cell/bead interface delivers a desensitizing signal that affects distal receptors (see Discussion). This general pattern of Ca^{2+} responses was observed in a large number of experiments in which several different IgE–FcεRI ligands were attached to the 6-μm beads. In particular, multivalent antigen (DNP-BGG, Fig. 1 *C*) and the anti-rat IgE mAb, A2 (11, 32) (Fig. 1 *D*) both elicited only transient Ca^{2+} responses when attached to beads at a variety of conjugation densities, even though fluorescence microscopy clearly showed a significant accumulation of IgE–FcεRI in the cell/bead interface for the former ligand, indicating an increased average density of FcεRI in that region (data not shown). As with soluble sAv added subsequently to cell/bead conjugate formation in Fig. 1 *B*, soluble DNP-BGG (Fig. 1 *C*) and A2 (Fig. 1 *D*) elicit moderately strong, sustained responses in both free cells and cell/bead conjugates, and the response for the conjugates is consistently reduced in magnitude relative to that of free cells.

The capacity of ligand-coated beads to stimulate downstream signaling events in RBL cells was further investigated by measuring exocytosis as represented by release of β-hexosaminidase (28). As shown in Fig. 2 *A*, addition of optimal doses of multivalent DNP-BSA or sAv to IgE_{biotin}-sensitized RBL cells in suspension causes β-hexosaminidase release. The magnitude of this response is substantially less than that for the same cells when they are spread on a plastic surface (21; Pierini, L., D. Holowka, and B. Baird, unpublished observations). Also shown in Fig. 2 *A* is the degranulation response to large (~100-μm diam) TNP-coated Sepharose 4B beads. Even at a small ratio of beads to cells (~1 bead/19 cells), these beads stimulate degranulation at least as well as that observed with soluble ligands. In contrast, relatively little degranulation is observed when 6-μm beads are added to form 1:1 conjugates with the cells (as determined by microscopic evaluation). Increasing the average ratio of beads attached per cell to 3:1 results in a slightly larger response that is still small relative to that observed with soluble ligands or with the 100-μm Sepharose beads.

Stronger degranulation responses can be elicited from both adherent and suspended RBL cells by treatment with cytochalasin D, which caps actin and inhibits microfilament polymerization (40, 47). As shown in Fig. 2 *B*, the

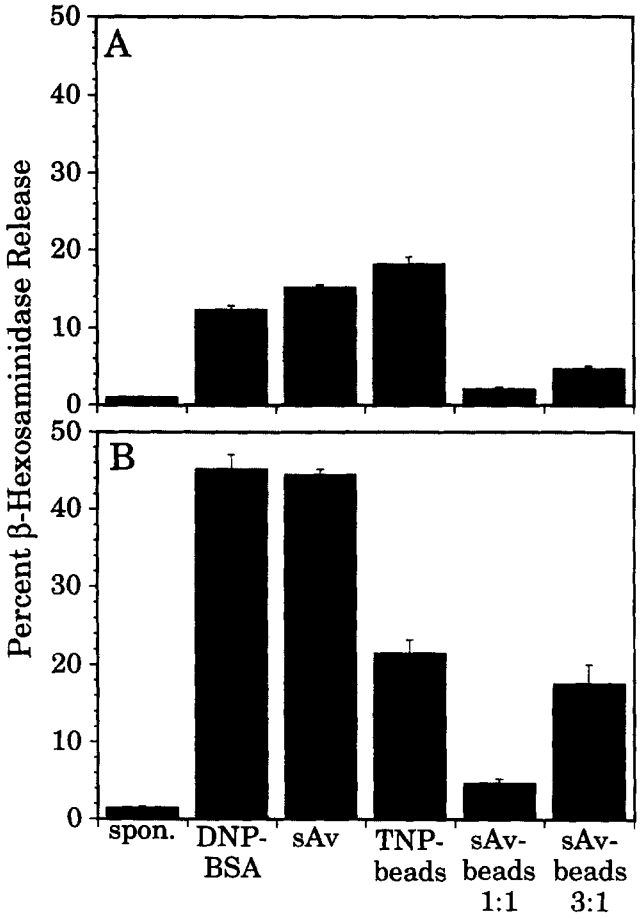

Figure 2. Degranulation responses of RBL cells to bead-bound and soluble ligands in the absence (*A*) and presence (*B*) of 2 μM cytochalasin D. Suspended RBL cells (1×10^6 cells/ml) sensitized with anti-DNP IgE_{biotin} were incubated at 37°C for 1 h with either 50 ng/ml DNP-BSA, 0.5 nM sAv, 2.5×10^4/ml TNP-sepharose beads, 2×10^6/ml sAv-coated 6-μm beads (1:1 conjugates), 6×10^6/ml sAv-coated 6-μm beads (3:1 bead/cell conjugates), or no ligand (spontaneous). At the end of the incubation, cells and beads were sedimented (9,000 *g*) and aliquots of the supernatants were analyzed for β-hexosaminidase release. Degranulation is given as the percent of total cellular β-hexosaminidase released. Error bars represent the standard deviation of duplicate samples from two separate experiments carried out on different days.

response to soluble cross-linking ligands by cytochalasin D–treated RBL cells in suspension is three- to fourfold larger than that in the absence of cytochalasin D. Under these conditions, the response to the TNP beads is only slightly greater than that in the absence of cytochalasin D. This is probably because cells attach less readily to the large TNP beads after treatment with cytochalasin D (data not shown). In the presence of cytochalasin D, sAv-conjugated 6-μm beads bound to cells in a 1:1 ratio do not trigger a significantly larger response than in the absence of cytochalasin D. Higher ratios of 6-μm beads bound per cell cause a more substantial response that is similar in magnitude to that elicited by TNP beads (Fig. 2 *B*). As for the large beads, the contact area between the cell and the 6-μm beads is reduced in the presence of cytochalasin D. In particular, cytochalasin D–treated cells do not appear to wrap around the 6-μm beads to as great an extent as untreated cells (data not shown). From these results we conclude that, in the presence of cytochalasin D, degranulation can be stimulated by the 6-μm beads when there is sufficient cell surface contact with the beads. In contrast, cell/bead conjugates in the absence of cytochalasin D fail to degranulate significantly, even when a substantial fraction of the cell surface area (and FcεRI) are in the contact region. These results suggest that the microfilament cytoskeleton plays a role in limiting the response of the cells to ligands attached to 6-μm beads (see below).

Membrane Components Are Excluded from the RBL Cell/6-μm Bead Interface but Not from the RBL Cell/TNP Bead Interface

To investigate why 6-μm beads are poor stimulators of Ca^{2+} and degranulation responses in RBL-2H3 cells, the distribution of potentially relevant plasma membrane proteins on cells conjugated to beads was evaluated with confocal fluorescence microscopy. Because our recent results have indicated that TX-100–resistant membrane domains (2) may play a role in FcεRI-mediated signaling (17), we initially determined whether markers for these domains are present at the cell/6-μm bead interface. Cells, labeled with FITC-IgE_{biotin} and with Cy3-labeled mAb specific either for the GPI-linked protein Thy-1 or for α-galactocyl derivatives of the ganglioside GD_{1b} (AA4), were mixed with 6-μm sAv-coated beads for 30 min at room temperature and then fixed and examined by confocal fluorescence microscopy. When focused at the equator of the cell, the FITC-IgE_{biotin} appears as a uniform ring stain (Fig. 3,

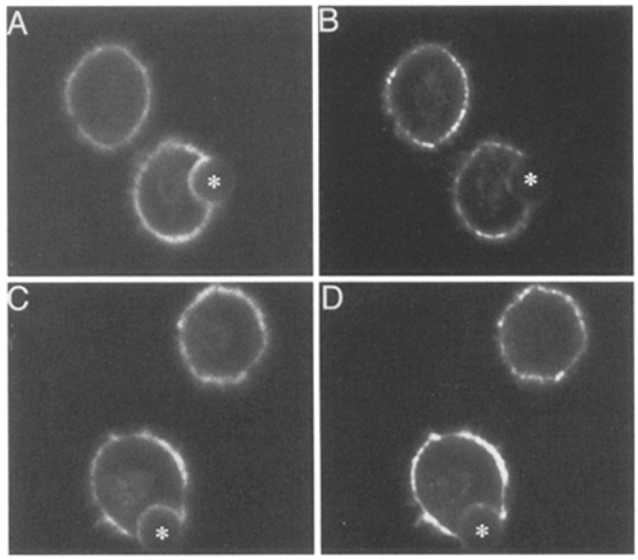

Figure 3. Confocal fluorescence microscopy of RBL cell/sAv bead conjugates shows exclusion of membrane components. RBL cells were sensitized with FITC-IgE_{biotin} and labeled with either Cy3-AA4 (*A* and *B*) or Cy3-Thy-1 (*C* and *D*) before being briefly plated onto coverslips. sAv beads (*) were added to the coverslips and allowed to interact with the cells for 30 min at room temperature. The cells were then formaldehyde fixed before imaging as described in Materials and Methods. FITC fluorescence is shown in *A* and *C*, and Cy3 fluorescence is shown in *B* and *D*. Bead diameter is 6 μm.

A and *C*), and the staining at the cell/bead interface is as bright or brighter than the rest of the membrane staining. As evident in these and subsequent images, FITC-IgE_{biotin} often extends at least part way around the bead, indicating the movement of the plasma membrane around the bead as expected during active engulfment. The same cell/bead conjugate in Fig. 3 *A* is shown in Fig. 3 *B* with the distribution of the ganglioside GD_{1b} made visible with Cy3-AA4. In contrast to the FITC-IgE_{biotin} (Fig. 3 *A*), the Cy3-AA4 (Fig. 3 *B*) is largely excluded from the cell/bead contact site. Outside of the contact site of cell/bead conjugates or on the surface of cells not attached to beads, the Cy3-AA4 is slightly patchy in appearance, possibly related to its interaction with detergent-resistant membrane domains (see below). Similarly to GD_{1b}, Thy-1, as visualized with Cy3-anti–Thy-1 (Fig. 3 *D*), is largely excluded from the contact site of cell/bead conjugates, whereas FITC-IgE_{biotin} is not (Fig. 3 *C*). Also, the distribution of Cy3-anti–Thy-1 label in other regions of the cell surface is more patchy than the corresponding distribution of FITC-IgE_{biotin}. These images are representative of the large majority of hundreds of conjugates examined during several independent experiments with each label.

Our recent results show that small amounts of IgE–FcεRI coisolate with TX-100–resistant membrane domains after cell lysis with TX-100 (17), and this amount increases significantly if IgE–FcεRI is first aggregated by external ligands. Therefore, we investigated whether FITC-labeled AA4, which binds to GD_{1b} and serves as a marker for the isolated domains, coredistributes on the cell surface with aggregated IgE–FcεRI. Fig. 4, *A* and *B*, show mostly uniform surface distributions for Cy3-IgE and FITC-AA4, respectively, when these are sequentially bound to RBL-2H3 cells at 37°C as previously described (37). As shown in Fig. 4, *C* and *D*, aggregation of Cy3-IgE by biotinylated anti-ε and sAv results in large-scale clustering of IgE–FcεRI at the cell surface and substantial coredistribution of FITC-AA4. This coredistribution was found to be dependent on binding of the AA4 mAb before FcεRI aggregation; cells labeled with FITC-AA4 subsequent to IgE–FcεRI aggregation and formaldehyde fixation showed a more uniform distribution of FITC-AA4 at the cell surface with little or no coincidence with aggregated IgE–FcεRI patches (data not shown). These results suggest that aggregation of the GD_{1b} gangliosides may be necessary for their stable association with the membrane domains (see Discussion). Furthermore, these results suggest that the exclusion of GD_{1b} and Thy-1 from the cell/bead interface (Fig. 3) may be due to general exclusion of detergent-resistant membrane domains and concomitant disruption of the interactions that normally occur between these domains and IgE–FcεRI aggregated by soluble cross-linkers.

We evaluated this possibility by examining the distribution of the carbocyanine lipid probes, $DiIC_{16}$ and fast DiI, under conditions of cell/bead conjugate formation. Our previous results indicated that $DiIC_{16}$ labels plasma membrane domains that separately coredistribute with aggregated IgE–FcεRI or GD_{1b} (49), and this suggests that $DiIC_{16}$ labels the detergent-resistant membrane domains on intact cells. Consistent with this possibility and the results of Fig. 3, we find that $DiIC_{16}$ is also largely excluded from the cell/6-μm bead interface. Fig. 5, *A–C*, shows representative images of cells labeled with FITC-IgE_{biotin} (Fig. 5 *A*) and $DiIC_{16}$ (Fig. 5 *B*). The interface between the bead and the cell is clearly depleted of $DiIC_{16}$ relative to the rest of the cell surface. Fig. 5 *C* shows the image in *B* thresholded as described in Materials and Methods to emphasize this difference.

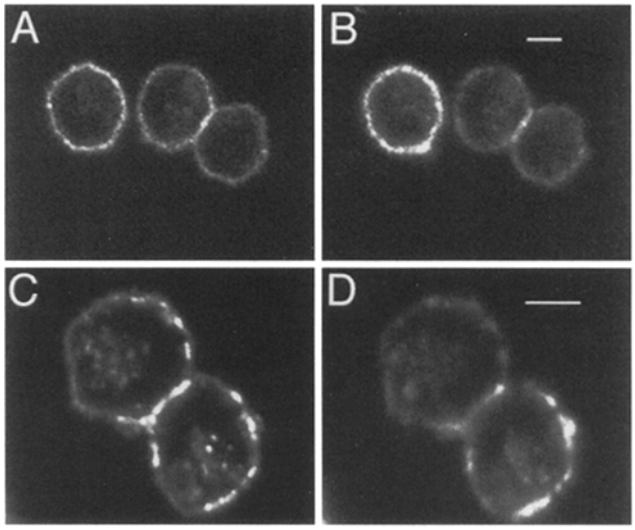

Figure 4. Aggregation of IgE–FcεRI complexes on RBL-2H3 mast cells by soluble cross-linking ligands causes coredistribution of a GD_{1b} ganglioside. RBL cells were sensitized with Cy3-conjugated IgE (visualized in *A* and *C*) before labeling with FITC-AA4 (visualized in *B* and *D*). To cross-link IgE–FcεRI, cells were treated with biotinylated sheep anti-IgE(ε), followed by streptavidin (*C* and *D*), whereas control cells were treated with streptavidin only (*A* and *B*). Bar, 5 μm.

$DiIC_{16}$ contains two saturated acyl chains and is expected to associate with TX-100–resistant membrane components by virtue of this structural feature (45). A structurally similar lipid probe, fast DiI, contains unsaturated acyl chains and is expected to associate less with the TX-100–resistant domains. Consistent with these expectations, fast DiI coredistributes with FcεRI aggregated by soluble cross-linking ligands to a lesser extent than $DiIC_{16}$ (Holowka, D., unpublished observations). As shown in Fig. 5, *D–F*, fast DiI is excluded from the cell/bead interface to a lesser extent than $DiIC_{16}$. Fig. 5 *F* shows the image in *E* thresholded identically to that in *C*, and it is clear that the cell/bead interface contains a larger amount of fast DiI relative to the surrounding plasma membrane than that seen for $DiIC_{16}$. We have observed that fast DiI labels intracellular membranes to a larger extent than $DiIC_{16}$, which is resistant to bilayer flip-flop (53), suggesting that the latter is retained in the outer leaflet of the plasma membrane, whereas the former more readily flips to the inner leaflet.

We next examined whether $p53/56^{lyn}$, an inner leaflet-associated component of TX-100–resistant membrane domains (17), is excluded from the cell/6-μm bead contact region. Fig. 6, *A* and *B*, compares the distribution of FITC-IgE to $p53/56^{lyn}$ labeled with a Cy3-conjugated secondary antibody after methanol fixation and binding of a polyclonal anti-lyn Ab. Similar to the results with Cy3-AA4, Cy3-anti–Thy-1, and $DiIC_{16}$, $p53/56^{lyn}$ is mostly excluded from the interface of cells and 6-μm beads (Fig. 6 *B*) but is

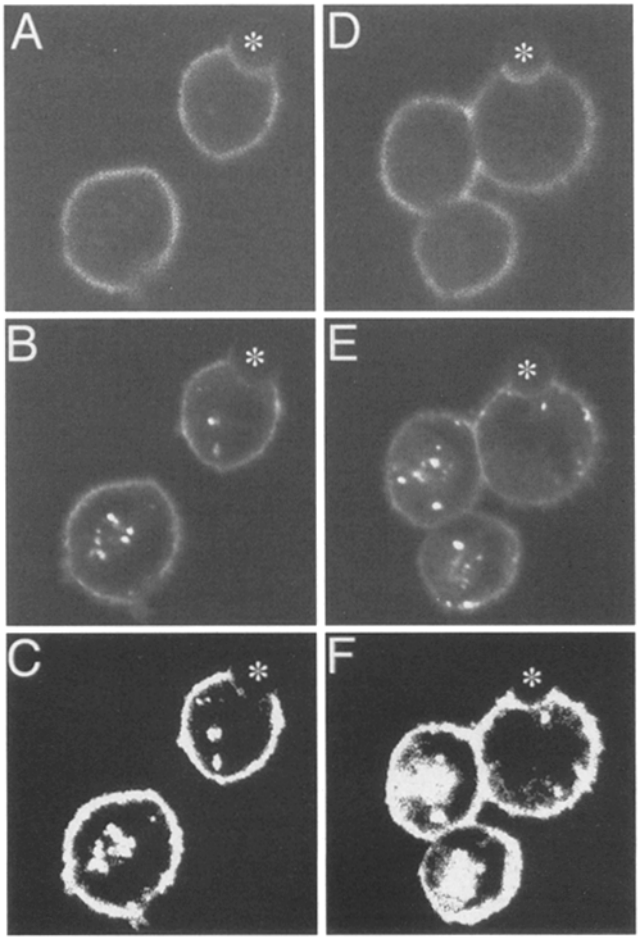

Figure 5. The lipophilic membrane probe $DiIC_{16}$, but not fast DiI, is excluded from the interface of cell/bead conjugates. The cells were sensitized with FITC-IgE_{biotin} (visualized in *A* and *D*) before labeling with either $DiIC_{16}$ (visualized in *B*) or fast-DiI (visualized in *E*). Streptavidin beads were added after the labeled cells were plated as described in Fig. 3. The images shown in *B* and *E* were thresholded as described in Materials and Methods to produce the images shown in *C* and *F*, respectively. All beads in these images are 6 μm in diameter.

fairly uniform elsewhere on the cell surface. $p53/56^{lyn}$ has been implicated in the earliest steps of FcεRI-mediated signal transduction (15, 44), and therefore its exclusion is potentially related to the lack of sustained Ca^{2+} responses or stimulated degranulation caused by ligand-coated beads.

Integrins are transmembrane heterodimeric proteins that appear to enhance the FcεRI-mediated responses in adherent RBL-2H3 cells (21), and they are known to colocalize with microfilaments at focal adhesion contacts (50). As shown in Fig. 6, *C* and *D*, a mAb specific for VLA4 integrin labels formaldehyde-fixed and permeabilized RBL-2H3 cells in suspension with a patchy surface fluorescence, and the cell/bead interface is largely devoid of VLA4 (Fig. 6 *D*). This representative image indicates that exclusion of membrane components is not selective for detergent-resistant membrane domain-associated components, as integrins do not cofractionate with TX-100–resistant membrane domains following cell lysis and sucrose gradient centrifugation (Field, K.A., D. Holowka, and B. Baird, unpublished results; 18).

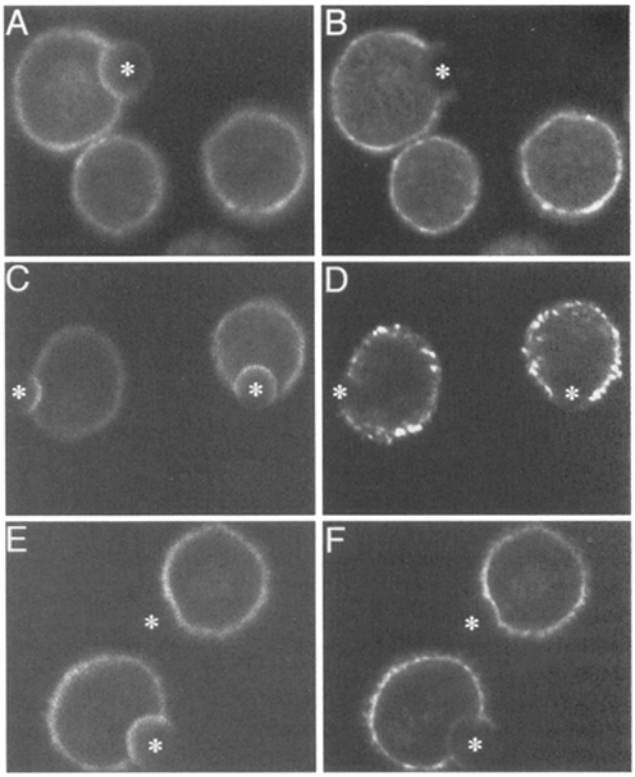

Figure 6. Confocal fluorescence microscopy of cell/sAv bead conjugates shows exclusion of $p53/56^{lyn}$ (*B*), VLA4 intergrin (*D*), and monomeric FcεRI (*F*) from the cell/bead interface. (*A–D*) Cell/bead conjugates were formed between sAv beads and FITC-IgE_{biotin}–sensitized RBL cells. FcεRI localization is visualized with the fluorescence of receptor-bound FITC-IgE_{biotin} (*A* and *C*), while $p53/56^{lyn}$ (*B*) and VLA4 (*D*) localization is visualized with indirect immunofluorescence of fixed and permeabilized cells. (*E* and *F*) Cells sensitized with a premixture of FITC-IgE_{biotin} and Cy3-IgE were conjugated to sAv beads as above. FITC-IgE_{biotin} (*E*) can become cross-linked by the sAv beads while the Cy3-IgE (*F*), which is not biotinylated, cannot. Bead diameter is 6 μm.

To test whether cytoskeletal attachment of integrins and membrane domains might mediate the exclusion of these components from the cell/bead contact site, we examined the distribution of monomeric Cy3-IgE–FcεRI complexes under conditions in which FITC-IgE_{biotin}–FcεRI are specifically recruited. Fig. 6, *E* and *F*, shows a representative pair of micrographs in which FITC-IgE_{biotin}–FcεRI exhibits the expected localization at the interface after cell/bead conjugation has been initiated (Fig. 6 *E*, *lower cell*). However, as seen in Fig. 6 *F* (*lower cell*), Cy3-IgE–FcεRI are mostly excluded from this interface, although a small amount of this label can be seen around the bead, especially at the leading edge of the plasma membrane extensions. The upper cell/bead conjugate in this micrograph shows the distribution of Cy3-IgE–FcεRI during the earliest stages of association, and it is evident that these monomeric complexes have not yet been excluded from the interface. These results suggest a more general mechanism for exclusion of plasma membrane components during this conjugation process, as there is good evidence that most monomeric IgE–FcεRI are not anchored to the cytoskeleton or other immobilizing structures even after the aggre-

gation of a separate population of these receptors on the same cell (31, 32).

To pursue the possibility that the exclusion of membrane domain components observed for cells conjugated to 6-μm beads is related to their compromised signaling, we examined whether the functionally competent TNP beads caused a similar exclusion. When these large TNP-Sepharose beads are mixed with RBL cells that have been sensitized with FITC-IgE, cells that form conjugates with the beads show some recruitment of FITC-IgE to the cell/bead interface (Fig. 7, *A* and *C*). Before the formation of these conjugates, the cells were labeled with the membrane domain markers Cy3-AA4 (Fig. 7 *B*), $DiIC_{16}$ (Fig. 7 *D*), or Cy3-anti–Thy-1 (data not shown). In contrast to the results with the cells conjugated to 6-μm beads, these membrane domain markers are not excluded from the interface, and they show enhanced labeling in this region in some cells (Fig. 7 *B*). As the TNP beads, but not the 6-μm beads, elicit a cellular response (Fig. 2), these results are consistent with the possibility that the interaction of IgE–FcεRI with membrane domains is involved in cellular activation.

RBL-2H3 Cells Phagocytose 6-μm Beads

As described above, these cells, mixed with ligand-coated 6-μm beads at room temperature for 30 min (conditions for confocal microscopy), appear to engulf the beads to some extent in most cases and to engulf them completely in some cases. Incubation of beads and cells at 37°C results in more rapid engulfment, such that after 20 min the majority of cells forming conjugates appeared to have engulfed their associated bead. As an illustration, Fig. 8 shows an equatorial view of two RBL cells that have completely or nearly completely engulfed sAv beads. The differential interference contrast (DIC) image in Fig. 8 *A* shows two cells that have each completely engulfed a bead, with one cell having only partially engulfed a second bead. The fluorescence image of these cells (Fig. 8 *B*) shows accumulation of receptor-associated FITC-IgE_{biotin} fluorescence around the partially engulfed bead, as seen in previous images (Figs. 3 and 6). The two beads that appear to be completely engulfed show dimmer fluorescence that completely surrounds the periphery of the bead. The dim fluorescence is apparently due to quenching of the fluorescein fluorescence within the acidic environment of the phagosome; the fluorescence quenching is reversed if the cells are permeabilized with TX-100 (data not shown). For cell/bead conjugates with reduced FITC fluorescence, visualization of receptor-bound FITC-IgE in both the *xy*- and the *yz*-planes shows that the bead is completely surrounded by cell membrane (data not shown). Under these conditions of cell/bead conjugation (20 min at 37°C), ~60% (n = 100) of the conjugates showed complete engulfment of the bead, whereas conjugates formed at 4°C or at 37°C in the presence of 2 μM cytochalasin D show engulfment of <4% of the cell-associated beads (data not shown). Furthermore, as expected, sAv beads are not pha-

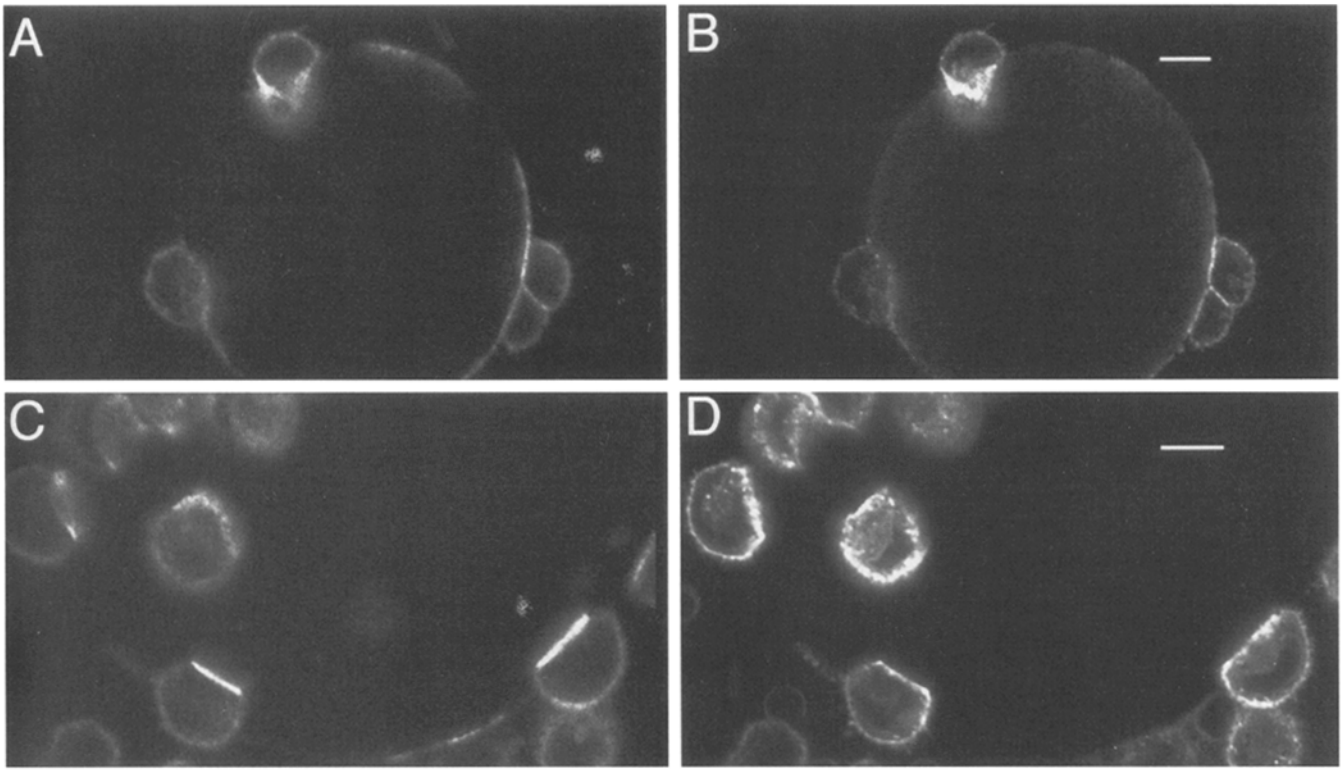

Figure 7. Membrane components are not excluded from the contact region of TNP bead/RBL cell conjugates. RBL cells were labeled with FITC-IgE then with either Cy3-AA4 (*A* and *B*) or $DiIC_{16}$ (*C* and *D*). Labeled cells were then mixed with TNP beads (~60-μm-diam sphere in *A* and *B*; ~80 μm hemisphere in *C* and *D*) for either 20 min on ice followed by a 10 min warm up at 37°C (*C* and *D*) or 20 min at room temperature with no further warm-up period (*A* and *B*). All samples were formaldehyde fixed before viewing. FITC fluorescence is shown in *A* and *C*, and Cy3 fluorescence is shown in *B* and *D*. Bars, 10 μm.

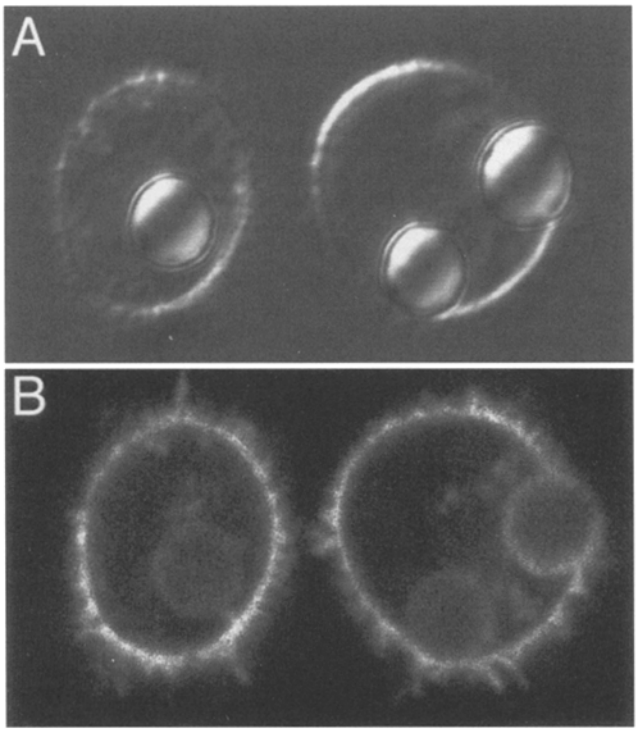

Figure 8. Phagocytosis of 6-μm beads by RBL cells. sAv beads were added to a suspension of FITC-IgE_{biotin}–sensitized cells and then mixed on a rotator for 20 min at 37°C. Both the differential interference contrast image (*A*) and the fluorescence image (*B*) show that the cells have completely engulfed two of the adherent beads. (Note that the completely engulfed beads show dimmer fluorescence than the partially engulfed bead.) Beads have diameters of 6 μm.

gocytosed by cells that have not been sensitized with IgE_{biotin} (data not shown). These observations indicate that 6-μm beads are undergoing FcεRI-mediated phagocytosis by the RBL cells because the process of phagocytosis requires the rearrangement of the actin assembly (1, 8) and does not occur at low temperatures (48).

The importance of stimulated actin polymerization in phagocytosis suggests that it may also be involved in excluding plasma membrane proteins at earlier stages of this process. Indeed, RBL-2H3 cells sensitized with IgE_{biotin} and treated with 2 μM cytochalasin D form conjugates with 6-μm sAv beads such that there is only limited surface area in contact with the beads and there is little or no exclusion of the ganglioside GD_{1b} (data not shown). To investigate directly whether microfilaments play a role in excluding membrane components from the cell/bead interface, we examined the distribution of polymerized actin during the early stages of the engulfment process with confocal microscopy of conjugates labeled with rhodamine-phalloidin. Fig. 9 shows a z-series from a single field containing a cell/bead conjugate in which sequential sections starting at the surface of attachment of the cell to the coverslip (*top left* to *right*). These sections reveal f-actin concentrated in the cell/bead contact region, as well as in the plasma membrane most proximal to this region. Sections farther from the the coverslip surface (*bottom left* to *right*) show where a larger amount of the bead has entered the cell, and the amount of f-actin staining is diminished relative to the adjacent plasma membrane. This pattern is consistent with the view that the microfilament-containing cytoskeleton is involved in clearing membrane components from the cell/bead interface and is, in turn, depleted from this region together with the membrane components as the bead enters the cell. Consistent with this view, we observe that fully engulfed beads do not have any detectable actin associated with them (data not shown).

Discussion

The results described in this study reveal an unexpected phenomenon: the clearance of several different components of the plasma membrane from the interface between RBL-2H3 mast cells and 6-μm beads that are conjugated specifically through IgE–FcεRI complexes. The exclusion process is initiated soon after conjugate formation and is virtually complete before the bead has been entirely ingested via phagocytosis. Cell/bead conjugates show exclusion at both room temperature and 37°C but not at 4°C, nor in the presence of cytochalasin D or in the absence of IgE. That is, exclusion does not occur under conditions that do not allow phagocytosis of the beads. It is unlikely that endocytosis is the main mechanism by which membrane components are cleared from the cell/bead interface, as we do not observe fluorescently labeled endosomal vesicles with any of the labeled antibodies under these conditions. Serial sections of rhodamine–phalloidin-stained cell/bead conjugates viewed with confocal microscopy suggest that microfilaments may be involved in the exclusion mechanism, but additional experiments are necessary to elucidate the molecular basis for this process. Notably, preliminary experiments showed that 6-μm beads coated with the anti-VLA4 mAb TA-2 also form conjugates efficiently and are phagocytosed by the RBL-2H3 cells, also causing exclusion of at least one membrane protein, FcεRI, from the contact region (Paar, J., and D. Holowka, unpublished results). This suggests that the protein clearance process is not specific for signaling mediated by aggregated FcεRI but rather is a more general feature of the phagocytosis process in these cells.

Our confocal microscopy studies were prompted by another unexpected result: ligand-coated 6-μm beads do not stimulate a sustained Ca^{2+} response from RBL cells under conditions in which the corresponding soluble ligands cause a strong, sustained response. This contrasts strikingly with our observation that these same 6-μm beads, when coated with an anti-TCR Ab, stimulate strong, sustained Ca^{2+} responses in the human T cell line, HPB-ALL (22; Fig. 1 *A*). The T cells are somewhat smaller than the RBL cells, and they do not appear to phagocytose the beads in these experiments (data not shown). RBL cells give only small, transient Ca^{2+} responses to bead-associated ligands regardless of the nature of the attached ligand (Fig. 1), despite the fact that there is considerable FcεRI cross-linking in at least some of these samples. In particular, DNP-BGG attached to these beads consistently caused enhanced FITC-IgE fluorescence at the cell/bead interface (data not shown) but failed to stimulate a sustained Ca^{2+} response (Fig. 1 *C*). Some preparations of sAv-coated beads also showed significant enhancement of FITC-IgE_{biotin} flu-

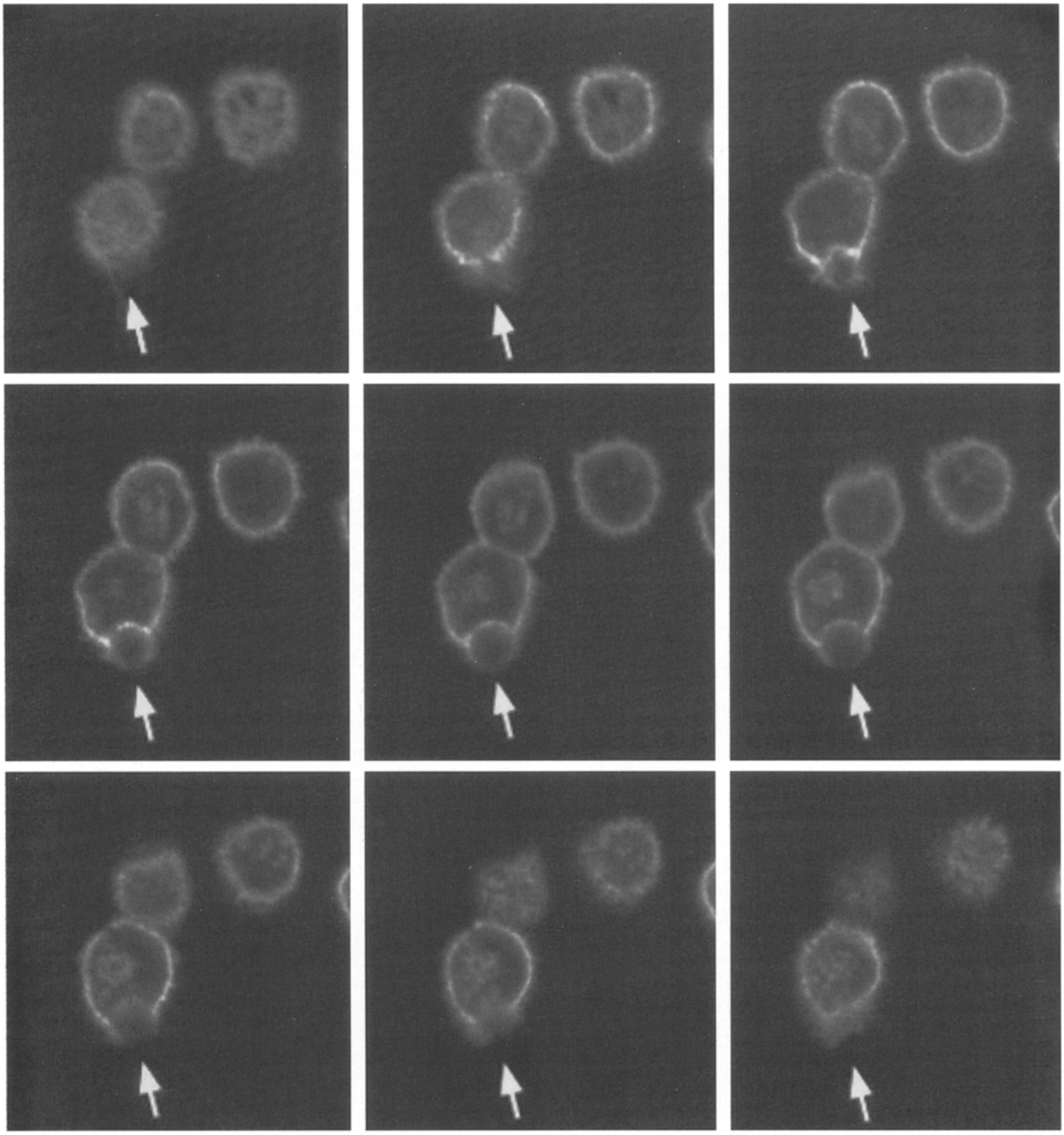

Figure 9. Accumulation of polymerized actin within the region of cell/bead contact. Cell/bead conjugates were formed by mixing sAv beads with IgE_{biotin}–sensitized cells for 30 min at room temperature. The cells were formaldehyde fixed, permeabilized with TX-100, and then labeled with rhodamine-phalloidin. The images represent a z-section series (0.6-μm steps) of three rhodamine-phalloidin–labeled cells, one of which is conjugated to a 6-μm bead. Sequentially higher sections are shown from left to right, beginning at the top left and ending at the lower right hand panel. Arrow indicates location of the bead. Bead diameter is 6 μm.

orescence at the cell/bead interface (Fig. 6, *C* and *E*, and data not shown). The results shown in Fig 6, *E* and *F*, make it clear that only ligand-attached IgE–FcεRI remain in the interfacial region during this process. Although the ligand-coated 6-μm beads do not deliver a strong stimulus, they do cause some desensitization as evidenced by the smaller secondary response to soluble ligands from cell/bead conjugates as compared to free cells (Fig. 1). The reduction of these secondary responses for cell/bead conjugates represents heterologous desensitization in that FcεRI outside of the cell/bead contact site are desensitized (in addition to those in the contact site). Analogous heter-

ologous desensitization was previously observed for FcεRI on RBL cells with soluble ligands (51). Because the 6-μm beads do cause some heterologous desensitization, this further indicates that the incapacity of these beads to stimulate RBL cells is not simply explained by insufficient FcεRI cross-linking.

The poor Ca^{2+} responses observed for cell/6-μm bead conjugates prompted us to examine the bead-mediated stimulation of degranulation. We found this was similarly deficient, even in the presence of cytochalasin D, which substantially enhances responses caused by soluble ligands. These results are consistent with the requirement for sustained elevation of cytoplasmic Ca^{2+} for degranulation in RBL cells (36). For other cell types, it has been shown that phagocytosis does not depend on a rise in cytoplasmic Ca^{2+} (13). In contrast to our results with 6-μm beads, large (~100 μm) TNP-derivatized Sepharose 4B beads can elicit significant degranulation responses from anti-DNP IgE-sensitized RBL cells. Similarly, RBL cells are productively stimulated by DNP-BGG– or DNP-BSA–coated polystyrene microtiter wells (data not shown), indicating that some presentations of surface-attached ligands do stimulate downstream signaling in RBL cells. Membrane components that are excluded from the interface of cell/6-μm bead conjugates are not excluded from the interface between TNP-derivatized beads and RBL cells. Thus, this exclusion correlates with the loss of downstream signaling in cell/6-μm bead conjugates.

$p53/56^{lyn}$ has been shown to participate in FcεRI-mediated signaling (15, 44). Therefore, the exclusion of most of the $p53/56^{lyn}$ from the cell/6-μm bead interface, and the consequent physical segregation of $p53/56^{lyn}$ from aggregated FcεRI, is likely to affect significantly the capacity of the 6-μm beads both to sustain Ca^{2+} mobilization and to stimulate degranulation. Specifically, $p53/56^{lyn}$ has been implicated in the phosphorylation of the tyrosines within the β- and γ-ITAM sequences (38, 43), and this process is halted in parallel with the Ca^{2+} and degranulation responses when antigen cross-linking is stopped by the addition of monovalent hapten (38). It will be interesting to determine the extent and time course of tyrosine phosphorylation that is stimulated by 6-μm beads under these conditions. A recent study indicated that the ITAM sequence in γ is important for activation of FcεRI-mediated phagocytosis in RBL-2H3 cells (12). A separate study in COS cells showed that a chimeric transmembrane protein containing an active catalytic domain of $p72^{syk}$ is sufficient to mediate phagocytosis of opsonized erthrocytes, despite the absence of detectable Ca^{2+} mobilization (19).

Exclusion from the cell/bead interface of several different components that we previously identified as markers for TX-100–resistant membrane domains, including α-galactocyl derivatives of the GD_{1b} ganglioside, GPI-linked Thy-1, and $DiIC_{16}$, as well as $p53/56^{lyn}$ (17, 49), suggests that these components may be excluded because of their association with the membrane domains. In particular, exclusion of $DiIC_{16}$, a lipid analogue that normally exhibits lipid-like lateral diffusion in the plasma membrane of RBL-2H3 cells (49), would be surprising if it were not associated with some larger complex that was excluded. Inefficient exclusion of fast DiI supports the role for membrane domains in $DiIC_{16}$ exclusion, as $DiIC_{16}$, with saturated acyl chains, is expected to associate with TX-100–resistant domains, whereas fast DiI, with unsaturated acyl chains, is not (45). It is also possible that the differential exclusion of fast DiI and $DiIC_{16}$ is related to their differential location in the inner and outer leaflets of the plasma membrane. Fast DiI more readily labels intracellular membranes and likely labels the inner leaflet of the plasma membrane to a greater extent than $DiIC_{16}$. However, the lack of extensive exclusion of fast DiI from the cell/6-μm bead contact site cannot be explained simply by location at the inner leaflet, as $p53/56^{lyn}$, also an inner leaflet component that is chiefly anchored by its myristoyl and palmitoyl acyl chains (42), is largely excluded. Accumulating evidence suggests that the interaction of aggregated FcεRI with the detergent-resistant membrane domains plays an important role in FcεRI-mediated signaling (17; Field, K.A., D. Holowka, and B. Baird, manuscript in preparation). The correlation of the loss of normal downstream signaling processes (Ca^{2+} mobilization and degranulation) with the exclusion of the membrane components, as demonstrated in this study, supports this hypothesis.

Transmembrane proteins are not generally coisolated with detergent-resistant membrane domains, consistent with the finding that self-association of saturated acyl chains provides the driving force for the formation of these structures (45). Nevertheless, we recently found that a large fraction of IgE_{biotin}–FcεRI complexes aggregated by soluble streptavidin associate with these domains when the detergent concentration used during lysis is sufficiently low (Field, K.A., D. Holowka, and B. Baird, manuscript in preparation). Under these conditions, only very small amounts of uncross-linked receptors associate with the isolated domains. Integrins have also been shown not to cofractionate with detergent-resistant membrane domains (18), and we have confirmed this observation with VLA4 on RBL cells (Field, K.A., D. Holowka, and B. Baird, manuscript in preparation). Despite this lack of association with the domains, both VLA4 and monomeric IgE–FcεRI are excluded from the cell/bead contact site, suggesting a more general mechanism for exclusion of these various membrane components. A role for the microfilament cytoskeleton in this process seems likely, and we have recent evidence that the detergent-resistant membrane domains interact with the actin cytoskeleton under some conditions (Holowka, D., C. Hine, and B. Baird. 1996. *FASEB J.* 10:A1215). If microfilament movement is involved in excluding membrane components, its effect on monomeric IgE–FcεRI is likely to be indirect. Thus, although our present results are consistent with an integral role for detergent-resistant membrane domains in normal FcεRI signaling, they could also be explained by microfilament-mediated exlusion of other important signaling molecules from the cell/bead interface.

The physiological role of the membrane component exclusion process is not yet completely clear, but it is evident that the initiation of phagocytosis by RBL cells diverts the normal downstream signaling pathways. Fusion of exocytotic granules with the internalized phagosome instead of their release to the extracellular medium is one possible consequence of this diversion. Previous studies indicated that microfilaments participate in phagocytosis (48), and selective exclusion of certain plasma membrane compo-

nents during the formation of phagosomes has been reported (10). In contrast to these results, the interaction of integrin-coated 12-μm beads with fibroblasts results in a massive accumulation of >20 different cytoskeletal and signaling proteins (35). Most phagocytosis studies are carried out at 37°C with macrophages and other professional phagocytes, and loss of microfilaments and associated proteins, as well as other plasma membrane components, generally is not found to be substantial until engulfment is complete (1). Our microscopic analysis at room temperature reveals that loss of membrane components and microfilaments from the cell/bead interface can occur before complete engulfment, but it is not yet clear whether the mechanism for this in RBL cells is similar to that in other phagocytic cells. Despite these questions, our present results establish that RBL-2H3 mast cells are capable of effectively segregating several different membrane proteins and lipids in a process that appears to involve the large-scale redistribution of these components in the two-dimensional plane of the plasma membrane. Furthermore, this process has rather dramatic effects on the downstream signaling pathways normally initiated by FcεRI aggregation. Future experiments will be aimed at understanding in greater detail the molecular mechanism of this process and its physiological ramifications.

We thank Dr. James P. Slattery of the Flow Cytometry and Imaging Facility of the Center for Advanced Technology and Biotechnology at Cornell University for assistance with the flow cytometry and confocal microscopy analyses and Dr. Reuben Siraganian of the National Institutes of Health (NIH, Bethesda, MD) for the AA4 mAb and for helpful discussions.

Supported by NIH grants AI2249 and GM08267 to L. Pierini.

Received 18 April 1996 and in revised form 2 July 1996.

References

1. Allen, L.H., and A. Aderem. 1995. A role for MARCKS, the alpha isozyme of protein kinase C and myosin I in zymosan phagocytosis by macrophages. *J. Exp. Med.* 182:829–840.
2. Anderson, R.G. 1993. Plasmalemmal caveolae and GPI-anchored membrane proteins. *Curr. Opin. Cell Biol.* 5:647–652.
3. Barsumian, E.L., C. Isersky, M.G. Petrino, and R.P. Siraganian. 1981. IgE-induced histamine release from rat basophilic leukemia cell lines: isolation of releasing and nonreleasing clones. *Eur. J. Immunol.* 11:317–323.
4. Basciano, L.K., E.H. Berenstein, L. Kmak, and R.P. Siraganian. 1986. Monoclonal antibodies that inhibit IgE binding. *J. Biol. Chem.* 261: 11823–11831.
5. Beaven, M.A., and H. Metzger. 1993. Signal transduction by Fc receptors: the Fc-epsilon-RI case. *Immunol. Today.* 14:222–226.
6. Benhamou, M., N.J. Ryba, H. Kihara, H. Nishikata, and R.P. Siraganian. 1993. Protein-tyrosine kinase p72syk in high affinity IgE receptor signaling. Identification as a component of pp72 and association with the receptor gamma chain after receptor aggregation. *J. Biol. Chem.* 268: 23318–23324.
7. Blank, U., C. Ra, L. Miller, K. White, H. Metzger, and J.P. Kinet. 1989. Complete structure and expression in transfected cells of the high affinity IgE receptor. *Nature (Lond.).* 337:187–189.
8. Brown, E.J. 1995. Phagocytosis. *Bioessays.* 17:109–117.
9. Cambier, J.C. 1995. Antigen and Fc receptor signaling. The awesome power of imunoreceptor tyrosine-based activation motif (ITAM). *J. Immunol.* 155(7):3281–3285.
10. Clemens, D.L., and M.A. Horwitz. 1992. Membrane sorting during phagocytosis: selective exclusion of major histocompatibility complex molecules but not complement receptor CR3 during conventional and coiling phagocytosis. *J. Exp. Med.* 175:1317–1326.
11. Conrad, D.H., E. Studer, J. Gervasoni, and T. Mohanakumar. 1983. Properties of two monoclonal antibodies directed against the Fc and Fab' regions of rat IgE. *Int. Arch. Allergy. Appl. Immunol.* 70:352–360.
12. Daeron, M., O. Malbec, C. Bonnerot, S. Latour, D.M. Segal, and W.H. Fridman. 1994. Tyrosine-containing activation motif-dependent phagocytosis in mast cells. *J. Immunol.* 152:783–792.
13. Di Virgilio, F., B.C. Meyer, S. Greenberg, and S.C. Siverstein. 1988. Fc receptor-mediated phagocytosis occurs in macrophages at exceedingly low cytosolic Ca^{2+} levels. *J. Cell Biol.* 106:657–666.
14. Draberova, L., and P. Draber. 1993. Thy-1 glycoprotein and src-like protein-tyrosine kinase p53/p56lyn are associated in large detergent-resistant complexes in rat basophilic leukemia cells. *Proc. Natl. Acad. Sci. USA.* 90:3611–3615.
15. Eiseman, E., and J.B. Bolen. 1992. Engagement of the high-affinity IgE receptor activates src protein-related tyrosine kinases. *Nature (Lond.).* 355: 78–80.
16. Erickson, J., P. Kane, B. Goldstein, D. Holowka, and B. Baird. 1986. Cross-linking of immunoglobulin E-receptor complexes at the cell surface: a fluorescence method for studying the binding of monovalent and bivalent haptens to immunoglobulin E. *Mol. Immunol.* 23:769–782.
17. Field, K.A., D. Holowka, and B. Baird. 1995. Fc epsilon RI-mediated recruitment of $p53/56^{lyn}$ to detergent-resistant membrane domains accompanies cellular signaling. *Proc. Natl. Acad. Sci. USA.* 92:9201–9205.
18. Fra, A.M, E. Williamson, K. Simons, and R.G. Parton. 1994. Detergent-insoluble glycolipid microdomains in lymphocytes in the absence of caveolae. *J. Biol. Chem.* 269:30745–30748.
19. Greenberg, S., P. Chang, D.C. Wang, R. Xavier, and B. Seed. 1996. Clustered syk tyrosine kinase domains trigger phagocytosis. *Proc. Natl. Acad. Sci. USA.* 93:1103–1107.
20. Guo, N.H., G.R. Her, V.N. Reinhold, M.J. Brennan, R.P. Siraganian, and V. Ginsburg. 1989. Monoclonal antibody AA4, which inhibits binding of IgE to high affinity receptors on rat basophilic leukemia cells, binds to novel alpha-galactosyl derivatives of ganglioside GD1b. *J. Biol. Chem.* 264:13267–13272.
21. Hamawy, M.M., C. Oliver, S.E. Mergenhagen, and R.P. Siraganian. 1992. Adherence of rat basophilic leukemia (RBL-2H3) cells to fibronectin-coated surfaces enhances secretion. *J. Immunol.* 149:615–621.
22. Hashemi, B.B., J.P. Slattery, D. Holowka, and B. Baird. 1996. Sustained T cell receptor-mediated Ca^{2+} responses rely on dynamic engagement of receptors. *J. Immunol.* 156:3660–3667.
23. Holowka, D., and B. Baird. 1992. Recent evidence for common signalling mechanisms among immunoreceptors that recognize foreign antigens. *Cell Signalling.* 4:339–349.
24. Holowka, D., and B. Baird. 1996. Antigen-mediated IgE receptor aggregation and signaling: a window on cell surface structure and dynamics. *Ann. Rev. Biophys. Biomol. Struct.* 25:79–112.
25. Holowka, D., and H. Metzger. 1982. Further characterization of the beta-component of the receptor for immunoglobulin E. *Mol. Immunol.* 19: 219–227.
26. Hutchcroft, J.E., R.L. Geahlen, G.G. Deanin, and J.M. Oliver. 1992. Fc-epsilon-RI-mediated tyrosine phosphorylation and activation of the 72-kda protein-tyrosine kinase ptk72 in RBL-2H3 rat tumor mast cells. *Proc. Natl. Acad. Sci. USA.* 89:9107–9111.
27. Issekutz, T.B., and A. Wykretowicz. 1991. Effect of a new monoclonal antibody, TA-2, that inhibits lymphocyte adherence to cytokine stimulated endothelium in the rat. *J. Immunol.* 147:109–116.
28. Kent, U.M., S.Y. Mao, C. Wofsy, B. Goldstein, S. Ross, and H. Metzger. 1994. Dynamics of signal transduction after aggregation of cell-surface receptors: studies on the type I receptor for IgE. *Proc. Natl. Acad. Sci. USA.* 91(8):3087–3091.
29. Lee, R.J., and J.M. Oliver. 1995. Roles for Ca^{2+} stores release and two Ca^{2+} influx pathways in the Fc epsilon R1-activated Ca^{2+} responses of RBL-2H3 mast cells. *Mol. Biol. Cell* 6:825–839.
30. Liu, F., J.W. Bohn, E.L. Ferry, H. Yamamoto, C. Molinaro, L. Sherman, N. Klinman, and D. Katz, 1980. Monoclonal dinitrophenol specific murine IgE antibody: purification, isolation, and characterization. *J. Immunol.* 124:2728–2736.
31. Mendoza, G., and H. Metzger. 1976. Distribution and valency of receptor for IgE on rodent mast cells and related tumour cells. *Nature (Lond.).* 264:548–550.
32. Menon, A.K., D. Holowka, W.W. Webb, and B. Baird. 1986. Cross-linking of receptor-bound IgE to aggregates larger than dimers leads to rapid immobilization. *J. Cell Biol.* 102(2):541–550.
33. Metcalfe, D.D., J.J. Costa, and P.R. Bard. 1992. Mast cells and basophils. *In* Inflammation: Basic Principles and Clinical Correlates. J.I. Gallin, I.M. Goldstein, and R. Snyderman, editors. Raven Press, Ltd., New York. 709–725.
34. Minoguchi, K., W.D. Swaim, E.H. Berenstein, and R.P. Siraganian. 1994. Src family tyrosine kinase $p53/56^{lyn}$, a serine kinase and Fc epsilon RI associate with alpha-galactosyl derivatives of ganglioside GD1b in rat basophilic leukemia RBL-2H3 cells. *J. Biol. Chem.* 269:5249–5254.
35. Miyamoto, S., H. Teramoto, O.A. Coso, J.S. Gutkind, P.D. Burbelo, and S.K. Akiyama. 1995. Integrin function: molecular hierarchies of cytoskeletal and signaling molecules. *J. Cell Biol.* 131:791–805.
36. Mohr, F.C., and C. Fewtrell. 1987. Depolarization of rat basophilic leukemia cells inhibits calcium uptake and exocytosis. *J. Cell Biol.* 104:783–792.
37. Oliver, C., N. Sahara, S. Kitani, A.R. Robbins, L.M. Mertz, and R. Siraganian. 1992. Binding of monoclonal antibody AA4 to gangliosides on rat basophilic leukemia cells produces changes similar to those seen with Fc-epsilon receptor activation. *J. Cell Biol.* 116:635–646.
38. Paolini, R., M.H. Jouvin, and J.P. Kinet. 1991. Phosphorylation and dephosphorylation of the high-affinity receptor for immunoglobulin E immediately after receptor engagement and disengagement. *Nature (Lond.).*

353:855–858.
39. Paolini, R., V. Renard, E. Vivier, K. Ochiai, M.H. Jouvin, B. Mallissen, and J.P. Kinet. 1995. Different roles for the Fc epsilon RI gamma chain as a function of the receptor context. *J. Exp. Med.* 181:247–255.
40. Pfeiffer, J.R., J.C. Seagrave, B.H. Davis, G.G. Deanin, and J.M. Oliver. 1985. Membrane and cytoskeletal changes associated with immunoglobulin E-mediated serotonin release from rat basophilic leukemia cells. *J. Cell Biol.* 101:2145–2155.
41. Pribluda, V.S., C. Pribluda, and H. Metzger. 1994. Transphosphorylation as the mechanism by which the high-affinity receptor for IgE is phosphorylated upon aggregation. *Proc. Natl. Acad. Sci. USA.* 91(23):11246–11250.
42. Resh, M.D. 1994. Myristylation and palmitylation of Src family members: the fats of the matter. *Cell.* 76:411–413.
43. Scharenberg, A.M., and J.P. Kinet. 1995. Early events in mast cell signal transduction. *Chem. Immunol.* 61:72–87.
44. Scharenberg, A.M., S. Lin, B. Cuenod, H. Yamamura, and J.P. Kinet. 1995. Reconstitution of interactions between tyrosine kinases and the high affinity IgE receptor which are controlled by receptor clustering. *EMBO (Eur. Mol. Biol. Organ.) J.* 14:3385–3394.
45. Schroeder, R., E. London, and D. Brown. 1994. Interactions between saturated acyl chains confer detergent resistance on lipids and glycosylphosphatidylinositol (GPI)-anchored proteins: GPI-anchored proteins in liposomes and cells show similar behavior. *Proc. Natl. Acad. Sci. USA.* 91: 12130–12134.
46. Schwartz, L.B., K.F. Austen, and S.I. Wasserman. 1979. Immunologic release of beta-hexosaminidase and beta-glucuronidase from purified rat serosal mast cells. *J. Immunol.* 123:1445–1450.
47. Seagrave, J., G.G. Deanin, J.C. Martin, B.H. David, and J.M. Oliver. 1987. DNP-phycobiliproteins fluorescent antigens to study dynamic properties of antigen-IgE-receptor complexes on RBL-2H3 rat mast cells. *Cytometry.* 8:287–295.
48. Silverstein, S.C., S. Greenberg, F. Di Virgilio, and T.H. Steinberg. 1989. Phagocytosis. *In* Fundamental Immunology. W.E. Paul, editor. Raven Press Ltd., New York. 703–720.
49. Thomas, J.L., D. Holowka, B. Baird, and W.W. Webb. 1994. Large-scale co-aggregation of fluorescent lipid probes with cell surface proteins. *J. Cell Biol.* 125:795–802.
50. Turner, C.E., and K. Burridge. 1991. Transmembrane molecular assemblies in cell–extracellular matrix interactions. *Curr. Opin. Cell Biol.* 3:849–853.
51. Weetall, M., D. Holowka, and B. Baird. 1993. Heterologous desensitization of the high affinity receptor for IgE, Fc-epsilon-RI, on RBL cells. *J. Immunol.* 150:4072–4083.
52. Weiss, A., and D.R. Littman. 1994. Signal transduction by lymphocyte antigen receptors. *Cell.* 76:263–274.
53. Wolf, D.E. 1985. Determination of the sidedness of carbocyanine dye labeling of membranes. *Biochemistry.* 24:582–586.